

# Ion and Water Transport Characteristics of Perfluorosulfonated Ionomer Membranes with $H^+$ and Alkali Metal Cations

Tatsuhiko Okada\*

National Institute of Advanced Industrial Science and Technology, Higashi 1-1-1, Central 5, Tsukuba, Ibaraki 305-8565, Japan

Hiroyuki Satou, Mitsuhiro Okuno, and Makoto Yuasa

Faculty of Science and Technology, Science University of Tokyo, 2641 Yamazaki, Noda, Chiba 278-8510, Japan

Received: August 17, 2001; In Final Form: November 17, 2001

Ion and water transport characteristics of Nafion ionomer membranes were investigated systematically in the mixed cation form of  $H^+$  and various kinds of alkali metal cation systems, which were prepared by equilibrating the membranes in the mixtures of HCl and alkali chloride in aqueous solutions of various mixing ratios. The membrane cationic composition showed that cations of larger atomic number had a higher affinity to sulfonic acid groups but less water content in the membrane than those of smaller atomic numbers. The net ionic conductivity was decreased, in any case, by the presence of alkali metal cations in the membrane. Different kinds of the interaction mode among cations were observed between H/Li or H/Na systems and H/K, H/Rb, or H/Cs systems. The interaction between alkali metal cations appeared to increase as the atomic number of the alkali metal cation increased. The water transference coefficient (electro-osmosis drag coefficient) increased from 2.5 to more than 10 by the presence of alkali metal cations. In the mixed systems, these cations were found to cause less water molecule drag than in the case of individual ions, in the presence of  $H^+$  ion. Overall, the transport characteristics of  $H^+$  and alkali metal cations influenced each other by way of the water molecules when they coexist in the membrane.

## 1. Introduction

Perfluorosulfonic acid polymer electrolyte membranes have attracted a lot of attention in the past decade because of their wide applications in chlor-alkali electrolysis, water electrolysis, polymer electrolyte fuel cells, and so on.<sup>1,2</sup> In fuel cell applications, newly synthesized membranes with lower costs are desired for practical purposes. The design concept would be extremely important in order to realize new membranes of high performances, especially high  $H^+$  conductivity. In this sense, elucidating the mechanism of transport of ions and water molecules in the membrane could greatly help such designing.

There have been a lot of performance evaluations of perfluorosulfonic acid polymer membranes for a single cation system, especially for H-form membranes.<sup>2–8</sup> However, the membrane characteristics of binary cation systems are found to provide more information than those of single cation systems.<sup>9–15</sup> Also, elucidating the mechanism of ion transport in mixed cation forms, in conjunction with water molecule transport, would be important for structural understanding of polymer electrolyte membranes. For this purpose, mixed cation systems are becoming very attractive because these systems would give much information about the ion–ion, ion–water, ion–polymer, and water–polymer interactions. Through such efforts, new polymer membranes of desired characteristics will be developed.

In this work, the transport and equilibrium properties of perfluorosulfonic acid polymer membranes are studied for H/Li, H/K, H/Rb, and H/Cs binary cation systems, in a systematic

way. The data are compared with those of the H/Na system, which is reported previously.<sup>16</sup>

## 2. Experimental and Calculations

**2.1. Membrane Preparation.** Nafion 115 and 117 of DuPont (Polymer Products Department, Wilmington, DE, nominal equivalent weight  $EW = 1100 \text{ g equiv}^{-1}$ ) were used as perfluorinated membrane specimens. The thicknesses of Nafion 115 and Nafion 117 membranes in the H-form were 125 and 175  $\mu\text{m}$  in the dry state and 160 and 220  $\mu\text{m}$  in the wet state, respectively. Membranes were cut into  $25 \times 25 \text{ mm}$  pieces, pretreated first in 2%  $H_2O_2$  at 80  $^\circ\text{C}$  for 2 h, immersed in 0.1  $\text{mol dm}^{-3}$  HCl for 24 h, and finally rinsed with pure water. Membranes were first stored in 0.03  $\text{mol dm}^{-3}$  HCl.

LiCl, KCl, RbCl, and CsCl were of reagent grade from Wako Pure Chemical Industries Ltd., Osaka, Japan, and used without further purification. HCl was from Merck Titrisol ampulae 1.000  $\text{mol dm}^{-3}$  (Merck, Darmstadt, Germany). Mixtures of solutions were prepared with various kinds of the equivalent fraction of HCl in the solution,  $x_{\text{HCl}} = 0.000, 0.0625, 0.158, 0.333, 0.529, 0.750, 0.871, 0.934, 0.967, 0.985$ , and 1.000, using deionized water. Here  $x_{\text{HCl}}$  is defined as  $x_{\text{HCl}} \equiv c_{\text{HCl}}/(c_{\text{HCl}} + c_{\text{ACl}})$  using the molar concentration of HCl and ACl ( $A^+ = \text{Li}^+, \text{K}^+, \text{Rb}^+$ , or  $\text{Cs}^+$ ),  $c_{\text{HCl}}$  and  $c_{\text{ACl}}$ , respectively, in the solution. The total concentration,  $c_{\text{HCl}} + c_{\text{ACl}}$ , was fixed to 0.03  $\text{mol dm}^{-3}$ .

Membranes were equilibrated in HCl/ACl ( $A^+ = \text{Li}^+, \text{K}^+, \text{Rb}^+$ , or  $\text{Cs}^+$ ) solutions of various compositions at 25  $^\circ\text{C}$ . During equilibration, solutions were renewed at least four times.

**2.2. Membrane Cationic Composition, Density, and Water Content.** The cationic composition of  $H^+$  in the membrane,  $x_{\text{HM}}$ , is defined as follows, using concentration of cations  $H^+$  and

\* Corresponding author. Fax: +81 298 61 4678. E-mail: okada.t@aist.go.jp.

$A^+$ ,  $c_{H^+}$  and  $c_{A^+}$ , respectively, in the membrane:

$$x_{HM} = \frac{c_{H^+}}{c_{H^+} + c_{A^+}} \quad (1)$$

Membranes in the dry state were analyzed by a Seiko Electric Co. model SEA2010 X-ray fluorescence spectroscopic analyzer, and the spectral intensity was counted for elements A ( $A = K, Rb, Cs$ ), S, and Cl. Element Cl was only within the error amount and was not further analyzed. The cationic composition of  $H^+$  in the membrane,  $x_{HM}$ , was calculated from the atomic ratio  $[A]/[S]$  in the spectra.

$$x_{HM} = 1 - \frac{[A]/[S]}{([A]/[S])_{x_{HCl}=0}} \quad (2)$$

where  $[A]$  and  $[S]$  are intensities of the elements A and S in the spectra, and the value in the denominator means the ratio  $[A]/[S]$  at  $x_{HCl} = 0$ . For the membrane with the H/K system, EPMA (electron probe microanalysis) was also employed for the  $K^+$  content determination using eq 2. A JEOL electron probe microanalyzer model JXA-8800M was used to obtain the energy dispersion spectra. The membrane samples were deposited with a thin layer of carbon in order to prevent the electric charging. For membranes with H/Li and H/K systems,  $Li^+$  or  $K^+$  were measured in the solution extracted by  $0.1 \text{ mol dm}^{-3}$  HCl using ICP (inductively coupled plasma emission spectrography, Thermo Jarrel Ash, model IRIS/AP).

The membrane water content was determined by the gravimetric method. First, the membrane sample was weighed in the wet state ( $W_{wet}$ ). The sample was then dried in a vacuum at room temperature for 24 h and then in a vacuum at  $110^\circ\text{C}$  for 12 h. After the sample was cooled in a desiccator, it was weighed ( $W_{dry}$ ), and from the weight difference the water content was calculated as the number of water molecules per cation exchange site  $\lambda \equiv n_{H_2O}/n_{SO_3^-}$ :

$$\lambda = \frac{(W_{wet} - W_{dry})EW'}{18W_{dry}} \quad (3)$$

where  $EW'$  is the equivalent weight value corrected for the exchanged cations  $A^+$  in place of  $H^+$ ,  $M_A$  being the atomic weight of the element A:

$$EW' \equiv EW + (M_A - 1)(1 - x_{HM}) \quad (4)$$

The density of the membrane in wet state,  $d_{wet}$  ( $\text{g cm}^{-3}$ ) was obtained in two ways. In the first method the mass of the wet membrane,  $W_{wet}$ , was divided by the volume in the wet state,  $V_{wet}$ , that was measured by a micrometer:

$$d_{wet} = W_{wet}/V_{wet} \quad (5)$$

In the second method the mass of membrane was measured in water, i.e.,  $W_{water}$ , and

$$d_{wet} = \frac{W_{wet}d_{water}}{W_{wet} - W_{water}} \quad (6)$$

where  $d_{water}$  ( $\text{g cm}^{-3}$ ) is the density of water.

**2.3. Membrane Conductivity.** The Teflon cell for impedance measurement of membranes was described elsewhere.<sup>17</sup> The impedance of the Nafion 117 membrane was measured in the lateral direction using a Solartron S-1260 frequency response analyzer (Solartron Instruments) with 20 mV ac modulation over

a frequency range from  $10^7$  to  $10^3$  Hz at the open-circuit potential at  $25^\circ\text{C}$ . The electrode was black-platinized Pt foil contacting the membrane on each of two sides with 10 mm width and 5 mm separation. During the measurement, the membrane was in contact with equilibrating solution by way of a  $10 \times 5$  mm window on each side. The specific conductivity of the membrane  $\kappa$  ( $\text{S cm}^{-1}$ ) was obtained from the real part of the impedance  $R$  ( $\Omega$ ) of the membrane:

$$\kappa = \frac{0.5}{Rl} \quad (7)$$

$l$  is the thickness (cm) of the membrane, which was measured for each sample.

**2.4. Ionic Transference Number.** The membrane-contact emf (electromotive force) method<sup>18</sup> was used where a pair of Nafion 117 membranes, each equilibrated with a solution of fixed ionic composition, were overlapped at one end, and the other ends were contacting the equilibrating solution with Ag/AgCl electrodes. This method was preferred to the Hittorf method for membrane stacks,<sup>19</sup> because of measuring time and precision.<sup>18</sup> Measurements were performed using a Teflon cell at  $25^\circ\text{C}$ , as described before.<sup>16</sup> Using the Gibbs–Duhem equation at isothermal and isopiestic conditions, and disregarding the chemical potential difference of  $H_2O$  at each side of the membrane for the present experimental setup, the emf  $E$  that arises as a result of the difference in chemical potentials of existing species across the membrane is expressed as follows:

$$\begin{aligned} E &= -\frac{1}{F}(t_{H^+}\Delta\mu_{HCl} + t_{A^+}\Delta\mu_{ACl}) \\ &= -\frac{1}{F}\left\{t_{H^+}\Delta\mu_{HCl} + t_{A^+}\left(-\frac{x_{HCl}}{x_{ACl}}\Delta\mu_{HCl}\right)\right\} \end{aligned} \quad (8)$$

where  $t_{H^+}$  and  $t_{A^+}$  are ionic transference numbers of  $H^+$  and  $A^+$  in the membrane, respectively, and  $\Delta\mu_{HCl}$  and  $\Delta\mu_{ACl}$  ( $\text{J mol}^{-1}$ ) are the difference in the chemical potentials of HCl and ACl, respectively, in two solutions contacting the membranes. The ionic transference number gives  $t_{H^+} + t_{A^+} = 1$ , and the solution composition  $x_{HCl} + x_{ACl} = 1$ , then the following equation results in

$$t_{H^+} = x_{HCl} - (1 - x_{HCl})\frac{d\Delta\phi}{d\Delta\mu_{HCl}} \quad (9)$$

where  $\Delta\phi \equiv EF$  ( $\text{J mol}^{-1}$ ) and  $F$  is the Faraday constant. The activity coefficients in determining  $\Delta\mu_{HCl}$  are calculated using Debye–Hückel equation.<sup>20,21</sup>

Mobility of ions in the membrane  $u_i$  ( $\text{m}^2 \text{V}^{-1} \text{s}^{-1}$ ) is obtained from the following equation:<sup>22</sup>

$$u_{H^+} = \frac{t_{H^+}\kappa}{Fc_{SO_3^-}x_{HM}} \quad (10)$$

$$u_{A^+} = \frac{(1 - t_{H^+})\kappa}{Fc_{SO_3^-}(1 - x_{HM})} \quad (11)$$

The concentration of sulfonic acid group in the membrane,  $c_{SO_3^-}$ , is expressed as follows:

$$c_{SO_3^-} = \frac{d_{dry}}{(EW')\chi_V} \quad (12)$$

where  $EW'$  is given by eq 4 and  $\chi_v$  is the ratio of membrane volume between the wet and dry states.

**2.5. Water Transference Coefficient.** The streaming potential method was utilized where the potential difference (emf) that arises as a result of a pressure difference  $\Delta p$  applied across the membrane contacting identical solutions on both sides was measured by a pair of Ag/AgCl electrodes.<sup>23</sup> The experiments were performed for Nafion 115 in deaerated solutions using a computer-aided homemade apparatus at 25 °C. Pressure was applied by N<sub>2</sub> gas with pressure control by model 250C-1-D of MKS Instruments, Inc.. Thereby emf was plotted against the square root of time.<sup>23</sup>

Two kinds of parameters, water transference coefficient,  $t_{H_2O}$ , and water permeability,  $L_p$  (m<sup>4</sup> J<sup>-1</sup> s<sup>-1</sup>), were obtained in a single measurement.  $t_{H_2O}$  arises due to the water movement associated with the charge transport, and  $L_p$  arises due to the pressure-driven flow of water in the membrane.<sup>23</sup> The emf is expressed by

$$EF = A - B\sqrt{t} \quad (13)$$

where the intercept and the slope of this line are given as follows:

$$A = -(t_{H^+}V_{HCl} + t_{A^+}V_{ACl} + t_{H_2O}V_{H_2O} + \Delta V_{el})\Delta p \quad (14)$$

$$B = -\frac{f}{F}L_p\Delta p \quad (15)$$

here  $V_i$  (cm<sup>3</sup> mol<sup>-1</sup>) is molar volume of species  $i$  and  $\Delta V_{el} \equiv V_{Ag} - V_{AgCl}$ . The amount of dissolved gas in the membrane is very small compared with other species and is neglected here. The following values were used for calculation:  $V_{HCl} = 18.3$ ,  $V_{LiCl} = 17.3$ ,  $V_{KCl} = 27.0$ ,  $V_{RbCl} = 32.3$ ,  $V_{CsCl} = 39.5$ ,  $V_{H_2O} = 18.0$ , and  $\Delta V_{el} = -15.5$ .<sup>18</sup>  $f$  is given by

$$f \equiv 4RT\pi^{-1/2} \left\{ [t_{H^+} - t_{H^+}(l)](D_{HCl}^{-1/2} - D_{ACl}^{-1/2}) + t_{Cl^-}(l) \left[ D_{ACl}^{-1/2} + \frac{c_{HCl}^0 D_{HCl}^{-1/2} + c_{ACl}^0 D_{ACl}^{-1/2}}{c_{HCl}^0 + c_{ACl}^0} \right] \right\} \quad (16)$$

for  $x_{HM} \neq 0$  and  $x_{HM} \neq 1$ , and

$$f \equiv 8RTt_{Cl^-}(l)(\pi D_{ACl})^{-1/2} \quad (17)$$

for  $x_{HM} = 0$ . Here  $t_i(l)$  is transference number of ion  $i$  in the solution, and  $c_i^0$  and  $D_i$  are the concentration and effective diffusion coefficient of electrolyte  $i$  in the solution phase, respectively. The literature values of  $D_i$  are  $D_{HCl} = 3.07 \times 10^{-9}$ ,  $D_{LiCl} = 1.280 \times 10^{-9}$ ,  $D_{NaCl} = 1.506 \times 10^{-9}$ ,  $D_{KCl} = 1.863 \times 10^{-9}$ ,  $D_{RbCl} = 2.02 \times 10^{-9}$ , and  $D_{CsCl} = 2.04 \times 10^{-9}$  m<sup>2</sup> s<sup>-1</sup>.<sup>21</sup>  $t_{H^+}$  is obtained by the measurements described in section 2.4.

### 3. Experimental Results

**3.1. Membrane Composition.** Figure 1 depicts the membrane cationic composition  $x_{HM}$  as a function of the contacting solution composition  $x_{HCl}$ , for membranes exchanged with four kinds of cation systems, H/Li, H/K, H/Rb, and H/Cs. Previous data for H/Na are also superimposed.<sup>16</sup> Different methods of analyses regarding the membrane composition gave very similar results within experimental uncertainties ( $\pm 5\%$  for X-ray fluorescence spectroscopy,  $\pm 8\%$  for EPMA, and  $\pm 10\%$  for the ICP method). In all cases except for the H/Li system, H<sup>+</sup> in Nafion membrane

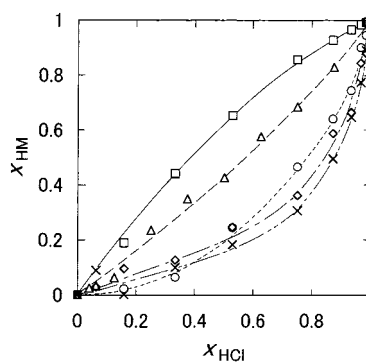


**Figure 1.** Membrane cationic composition  $x_{HM}$  at equilibrium state vs solution composition  $x_{HCl}$  for Nafion 117 at 25 °C: ( $\square$ ) H/Li system; ( $\Delta$ ) H/Na system (data from ref 16); ( $\circ$ ) H/K system; ( $\diamond$ ) H/Rb system; ( $\times$ ) H/Cs system.

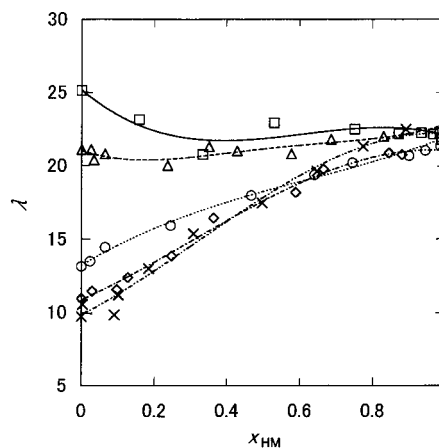


**Figure 2.** Membrane water content  $\lambda \equiv n_{H_2O}/n_{SO_3^-}$  plotted against membrane cationic composition  $x_{HM}$  for Nafion 117. Symbols are the same as in Figure 1.

was preferentially exchanged with any kind of foreign cations tested. The equilibrium constant  $K_{ex}$  of the exchange reaction between the solution phase and the membrane phase,  $HCl(aq) + AM = ACl(aq) + HM$  ( $A^+ = Li^+, K^+, Rb^+, Cs^+$ ), where  $M$  denotes the cation exchange site, is defined as follows:

$$K_{ex} = \frac{x_{ACl}x_{HM}}{x_{HCl}x_{AM}} \quad (18)$$

$K_{ex}$  is calculated to be  $1.85 \pm 0.16$  for H/Li,  $0.73 \pm 0.17$  for H/Na,  $0.25 \pm 0.06$  for H/K,  $0.20 \pm 0.07$  for H/Rb, and  $0.14 \pm 0.07$  for H/Cs systems, respectively.

It is observed two kinds of trends in Figure 1. First, cations of higher atomic number have higher affinity to the membrane than those of lower atomic numbers. These observations are in agreement with the results measured for Nafion 120 membranes.<sup>9,10</sup> Li<sup>+</sup> is a special ion and has almost no preference over H<sup>+</sup> in the membrane. Second, for H/Rb and H/Cs systems, a clear tendency is observed at the low H<sup>+</sup> content that the equilibrium isotherm is no longer concave but shows a sigmoid-shaped portion. This is indicative of some sort of interactions (repulsion) between cations, when the fraction of Rb<sup>+</sup> or Cs<sup>+</sup> is high in the membrane.

Figure 2 shows the water content in the membrane  $\lambda$  as a function of membrane cationic composition  $x_{HM}$  for various kinds of cation systems. Here the trend is also categorized into two classes of cations: one is for the Li<sup>+</sup> or Na<sup>+</sup> cation where  $\lambda$  does not change largely, and the other is for the K<sup>+</sup>, Rb<sup>+</sup>, or Cs<sup>+</sup> cation, where  $\lambda$  decreases largely by the presence of these

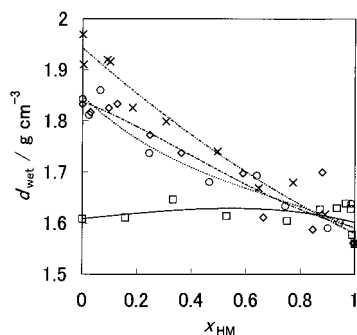


**Figure 3.** Density of the Nafion 117 membrane in the wet state plotted against membrane cationic composition  $x_{\text{HM}}$ . Symbols are the same as in Figure 1.

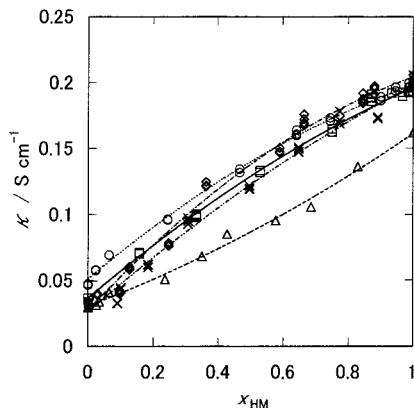


**Figure 4.** Membrane ionic conductivity  $\kappa$  in fully hydrated state plotted against membrane cationic composition  $x_{\text{HM}}$  for Nafion 115. Symbols are the same as in Figure 1.

cations. This trend was consistent with the trend observed in membrane cationic compositions, i.e., membranes exchanged with cations of higher affinity show lower water content.

In Figure 3, the density of the membrane in the wet state is shown against the membrane composition  $x_{\text{HM}}$ . Different methods of measuring the density gave almost the same results within experimental errors of  $\pm 2\%$ . For H/K, H/Rb, and H/Cs systems, the density increased almost linearly with the composition of foreign cations, when the membranes were exchanged with these cations, in contrast to the system H/Li where the density remained almost unchanged.

**3.2. Membrane Ionic Conductivity.** The membrane specific conductivity  $\kappa$  is plotted against the membrane cationic composition  $x_{\text{HM}}$  in Figure 4. In all cases,  $\kappa$  changed almost in a convex fashion with  $x_{\text{HM}}$ , with the exception that in the H/Li and H/Na systems,  $\kappa$  changed almost linearly. These different trends would typically show different effects about cation movements for mixed cation systems inside the membrane.

The mobility of cations calculated using eqs 10 and 11 together with the data of ionic transference numbers (see below) is plotted in Figure 5, as a function of membrane cationic composition  $x_{\text{HM}}$ . The mobility of  $\text{H}^+$  in the pure state was 6–9 times larger than that of  $\text{Li}^+$ ,  $\text{Na}^+$ ,  $\text{K}^+$ ,  $\text{Rb}^+$ , or  $\text{Cs}^+$ .

**3.3. Ionic Transference Number in the Membrane.** Figure 6 depicts the ionic transference number of  $\text{H}^+$  in the membrane  $t_{\text{H}^+}$ , plotted against the membrane cationic composition  $x_{\text{HM}}$ . In all cases,  $t_{\text{H}^+}$  decreased largely as  $x_{\text{HM}}$  becomes less than 0.5. The difference in the  $t_{\text{H}^+}$  vs  $x_{\text{HM}}$  dependence for different cation systems was small except for the H/Na system.

**3.4. Water Transference Coefficient and Water Permeability.** In Figure 7, the water transference coefficient  $t_{\text{H}_2\text{O}}$  is shown as a function of membrane cationic composition  $x_{\text{HM}}$ .

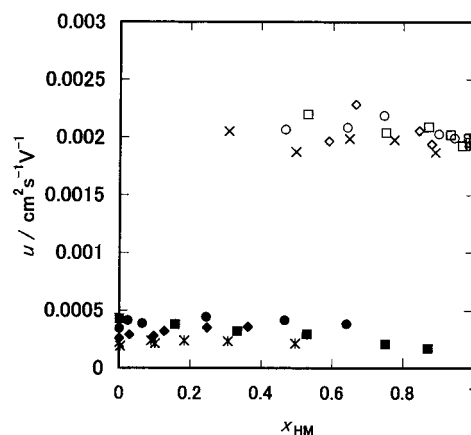


**Figure 5.** Mobility of cationic species in the membrane plotted against membrane cationic composition  $x_{\text{HM}}$ : ( $\square$ ,  $\blacksquare$ )  $u_{\text{H}^+}$  and  $u_{\text{Li}^+}$  in H/Li system; ( $\circ$ ,  $\bullet$ )  $u_{\text{H}^+}$  and  $u_{\text{K}^+}$  in H/K system; ( $\blacklozenge$ ,  $\blacktriangledown$ )  $u_{\text{H}^+}$  and  $u_{\text{Rb}^+}$  in H/Rb system; ( $\times$ ,  $*$ )  $u_{\text{H}^+}$  and  $u_{\text{Cs}^+}$  in H/Cs system.

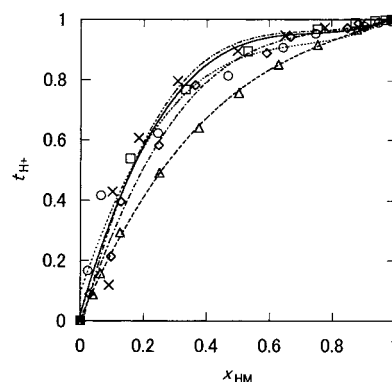


**Figure 6.** Ionic transference number of  $\text{H}^+$  in the membrane  $t_{\text{H}^+}$  for various cationic systems of Nafion 117, plotted against membrane cationic composition  $x_{\text{HM}}$ . Symbols are the same as in Figure 1.

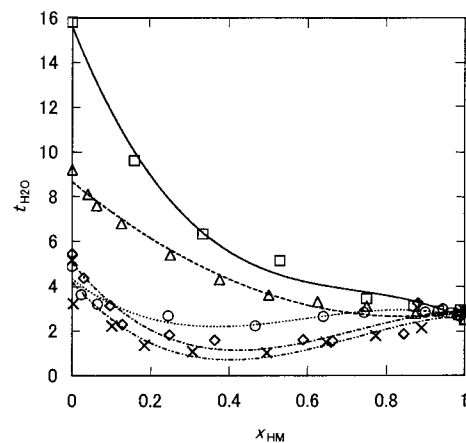
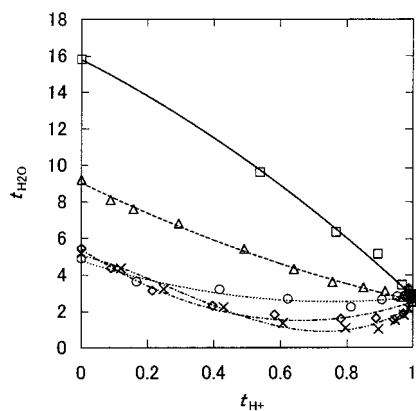


**Figure 7.** Water transference coefficient  $t_{\text{H}_2\text{O}}$  for various cationic systems of Nafion 115, plotted against membrane cationic composition  $x_{\text{HM}}$ . Symbols are the same as in Figure 1.

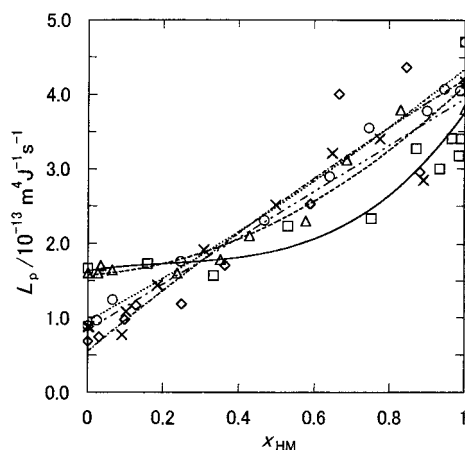
Depending on the system,  $t_{\text{H}_2\text{O}}$  vs  $x_{\text{HM}}$  curves appeared differently. For the H/Li system,  $t_{\text{H}_2\text{O}}$  increases sharply when  $x_{\text{HM}}$  was less than 0.5. For H/Rb and H/Cs systems, minima appeared in the curves. This could be ascribed to the possible interactions between  $\text{H}^+$  and alkali cations in these systems, when water was dragged in the mixed cation systems.

Figure 8 shows the plot of  $t_{\text{H}_2\text{O}}$  against the ionic transference number  $t_{\text{H}^+}$ .  $t_{\text{H}_2\text{O}}$  changes in different ways with  $t_{\text{H}^+}$ , depending on the alkali cations. In the case of H/Li and H/Na systems,  $t_{\text{H}_2\text{O}}$  changes almost linearly with  $t_{\text{H}^+}$ , but in the case of H/K,





**Figure 8.** Water transference coefficient  $t_{\text{H}_2\text{O}}$  vs ionic transference number of  $\text{H}^+$  in the membrane  $t_{\text{H}^+}$  for various cationic systems. Symbols are the same as in Figure 1.



**Figure 9.** Dependence of water permeability  $L_p$  of Nafion 115 on membrane cationic composition  $x_{\text{HM}}$ . Symbols are the same as in Figure 1.

H/Rb, and H/Cs systems,  $t_{\text{H}_2\text{O}}$  changes in the concave fashion. This means that in the latter case the total number of water molecules carried along with cations inside the membrane in mixed cation forms becomes smaller than that of the sum of the contribution from individual cations.

Water permeability  $L_p$  of Nafion 115 as calculated from eq 15 is shown in Figure 9 as a function of  $x_{\text{HM}}$ .  $L_p$  decreased largely as the alkali metal cations entered into H-form membranes. It is shown that the diffusion coefficient of water in the membrane,  $D_{\text{H}_2\text{O}}$ , is directly related to  $L_p$ ,<sup>16</sup> and in this context Figure 9 indicates that  $D_{\text{H}_2\text{O}}$  decreases almost to one-fifth when alkali metal cations enter into the membrane. This result, together with the increase in  $t_{\text{H}_2\text{O}}$  by the presence of such cations, poses a problem of membrane dehydration when the membrane is contaminated by impurity cations in the fuel cell application.<sup>16,22</sup> There is observed a difference in the manner  $L_p$  changes with the membrane cationic composition. For H/Li and H/Na systems, it is in a concave fashion, and for H/K, H/Rb, and H/Cs systems, it is almost in a linear fashion.

#### 4. Discussion

It is interesting to note the trend that when membranes are exchanged with cations of larger affinity to the sulfonic acid group, the ionic conductivity becomes smaller. The mobility of alkali metal cations changed in the following order:  $\text{Li}^+ < \text{Na}^+ > \text{K}^+ > \text{Rb}^+ > \text{Cs}^+$ , which is the order opposite to that of the affinity of the cation to the cation exchange sites except for  $\text{Li}^+$  (see also the  $K_{\text{ex}}$  values calculated from Figure 1). Cation

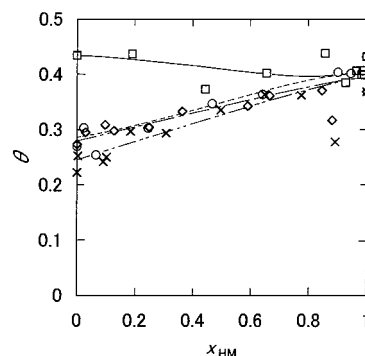


**Figure 10.** Volume fraction of water in the membrane  $\theta$  plotted against the membrane composition  $x_{\text{HM}}$ . Symbols are the same as in Figure 1.

selectivity and self-diffusion coefficients were closely connected through water uptake of the membrane, i.e., the degree of hydration of cations.<sup>24</sup> Yeager et al. related the cation selectivity of the membrane to the positive entropy change associated with the water release that occurs when  $\text{H}^+$  is replaced with  $\text{A}^+$ .<sup>9,10</sup> Also, Pintauro et al. interpreted the cation selectivity as the electrostatic interactions between cations and cation exchange sites together with the repulsive energy due to hydration effects.<sup>11,14</sup> In either case, stronger affinity of the cation to the sulfonic acid site may indicate stronger electrostatic interaction between the cation and the anionic groups, which results in lower mobility of cations.

The mobility of the cation follows the same order as in the water content ( $\text{Li}^+$  is the only exception). The same trend was reported for Nafion 117 and for poly(styrenesulfonate) membranes and was explained by the tortuosity effect.<sup>7,12,25</sup> In perfluorosulfonated ionomer membranes, a microstructural change of the polymer with ion and water clustering<sup>10</sup> might account for the difference in the mobility of cations. Seeing the results of water content and membrane density, the membrane appears to shrink when it is exchanged with  $\text{K}^+$ ,  $\text{Rb}^+$ , or  $\text{Cs}^+$  cations. Figure 10 depicts the volume fraction of water in the polymer  $\theta$  against  $x_{\text{HM}}$ , as determined by the volume of the membrane in dry and wet states ( $V_{\text{dry}}$  and  $V_{\text{wet}}$ , respectively):

$$\theta = \frac{V_{\text{wet}} - V_{\text{dry}}}{V_{\text{wet}}} \quad (19)$$

Note that  $\text{K}^+$ ,  $\text{Rb}^+$ , or  $\text{Cs}^+$  cations are all less hydrophilic than  $\text{H}^+$  and cause fewer amounts of water molecules inside the membrane as compared with  $\text{H}^+$ .<sup>10</sup> This would result in the smaller volume of hydrophilic domains inside the membrane and higher density of the membrane by shrinkage of the overall volume. The smaller domain of the ion conducting path will accordingly give rise to the lower ionic mobility. Similar results were observed in other cation systems.<sup>22,26</sup>  $\text{Li}^+$  was an exception, and the  $\theta$  vs  $x_{\text{HM}}$  curve differed markedly from that of  $\text{K}^+$ , although the mobilities were similar between  $\text{Li}^+$  and  $\text{K}^+$ .

It seems that there exist some interactions between cationic species in the membrane. Figure 1 indicates some interactions between the cationic species for  $\text{Rb}^+$  or  $\text{Cs}^+$  cations, when the population of these cations is high. Also the convex fashion in the conductivity vs membrane cationic composition curves in Figure 4 for H/K, H/Rb, and H/Cs systems may indicate a slight acceleration mode when these ions coexist in the membrane. Figure 8 reveals that in the case of H/K, H/Rb, and H/Cs systems, the number of water molecules carried away by cations in the mixed state in the membrane varies depending on which cations exist inside.

The interaction between neighboring cations on the cation exchange sites can be discussed on the basis of the cation mixing process in the membrane. For a system of monovalent–monovalent cations in the membrane, HM and AM, the thermodynamic equilibrium constant,  $K_{th}$ , is defined for the reaction  $HCl(aq) + AM = ACl(aq) + HM$  as follows:<sup>27</sup>

$$K_{th} = \frac{a_{ACl}a_{HM}}{a_{HCl}a_{AM}} = K' \frac{\gamma_{HM}}{\gamma_{AM}} \quad (20.1)$$

$$K' \equiv \frac{a_{ACl}x_{HM}}{a_{HCl}x_{AM}} \quad (20.2)$$

where  $a_{HCl}$  and  $a_{ACl}$  are the activity of HCl and ACl in the solution, respectively, and  $\gamma_{HM}$  and  $\gamma_{AM}$  are activity coefficients of HM and AM in the membrane, respectively. It should be noted that  $K_{ex}$  (eq 18) is expressed straightforwardly by the ionic fraction, while  $K_{th}$  is expressed by the activity of species, and therefore has thermodynamic meaning. The Gibbs energy change for the exchange reaction is given as follows, using the chemical potential of relevant species:

$$\Delta G = \mu_{HM} + \mu_{ACl} - \mu_{HCl} - \mu_{AM} \quad (21)$$

which is 0 at the equilibrium state. Consider the standard state, where the activity coefficients of all the species are 1 and  $\mu_i$  becomes  $\mu_i^0$ . In this case  $\Delta G$  becomes  $\Delta G^0 = -RT \ln K_{th}$ , and

$$\Delta\mu_{HM} + \Delta\mu_{ACl} - \Delta\mu_{HCl} - \Delta\mu_{AM} = RT \ln K_{th} \quad (22)$$

where  $\Delta\mu_i \equiv \mu_i - \mu_i^0 = RT \ln a_i$ . Suppose  $x_{HM}$  equivalent of HM and  $x_{AM}$  equivalent of AM are brought together to make a mixture of H/A-form membrane. The Gibbs energy change of mixing,  $\Delta G_{mix}$ , follows:

$$\Delta G_{mix} = x_{HM}\Delta\mu_{HM} + (1 - x_{HM})\Delta\mu_{AM} \quad (23)$$

Differentiating eq 23 with respect to  $x_{HM}$  results in, with the help of the Gibbs–Duhem relationship,

$$\frac{d\Delta G_{mix}}{dx_{HM}} = \Delta\mu_{HM} - \Delta\mu_{AM} \quad (24)$$

Then it is obtained from eqs 20 and 22

$$\frac{d\Delta G_{mix}}{dx_{HM}} = RT \ln K_{th} - RT \ln K' + RT \ln \frac{x_{HM}}{x_{AM}} \quad (25)$$

According to the cell model of the HM and AM system of cation exchange membranes, the entropy of mixing,  $\Delta S_{mix}$ , and the enthalpy of mixing,  $\Delta H_{mix}$ , are given as follows:<sup>28</sup>

$$\Delta S_{mix} = -R(x_{HM} \ln x_{HM} + x_{AM} \ln x_{AM}) \quad (26)$$

$$\Delta H_{mix} = bx_{HM}x_{AM} \quad (27)$$

where  $b$  is a constant expressing the energy change of interaction between cation pairs through the mixing process. Hence

$$\begin{aligned} \frac{d\Delta H_{mix}}{dx_{HM}} &= RT(\ln K_{th} - \ln K') \\ &= b(1 - 2x_{HM}) \end{aligned} \quad (28)$$

Equation 28 indicates that if the mixture of HM and AM can be described by a regular mixture model, then the plot of  $\ln K'$

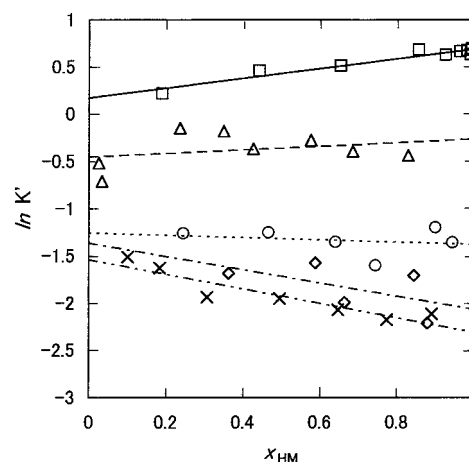


**Figure 11.** Relations between  $\ln K'$  and the membrane cationic composition  $x_{HM}$ . Symbols are the same as in Figure 1.

**TABLE 1: Cation Interactions in Nafion 117 Membranes<sup>a</sup>**

systems	A	B	$K_{th}$	$b/J \text{ mol}^{-1}$	$K'(x_{HM}=0.5)^9$
H/Li	0.17 <sub>2</sub>	0.51 <sub>7</sub>	1.54	641	1.71
H/Na	-0.45 <sub>3</sub>	0.18 <sub>9</sub>	0.70	235	0.85
H/K	-1.25 <sub>6</sub>	-0.12 <sub>1</sub>	0.27	-151	0.29
H/Rb	-1.36 <sub>2</sub>	-0.70 <sub>4</sub>	0.18	-873	0.21
H/Cs	-1.53 <sub>8</sub>	-0.76 <sub>9</sub>	0.15	-954	0.14

<sup>a</sup>  $K_{th}$ : thermodynamic equilibrium constant.  $b$ : constant expressing the interaction between  $H^+$  and  $A^+$  ( $A^+ = Li^+, Na^+, K^+, Rb^+, Cs^+$ ) as compared with the  $H^+-H^+$  and  $A^+-A^+$  pairs in the membrane (see eq 27).  $A$  and  $B$  are the intercept and the slopes of the lines in Figure 11, respectively ( $A = \ln K_{th} - b/RT$ ,  $B = 2b/RT$ ).  $K'(x_{HM}=0.5)$ : data for Nafion 120 in expanded form, calculated from ref 9.

against  $x_{HM}$  will result in a straight line.<sup>28</sup> Figure 11 depicts this plot for H/Li-, H/Na-, H/K-, H/Rb-, and H/Cs-form membrane systems. Here the activity of HCl and ACl in the solution,  $a_{HCl}$  and  $a_{ACl}$ , respectively, are calculated by the Debye–Hückel equation.<sup>21</sup> A good linearity indicates that  $H^+$  and other cations behave as if they are sitting on the cation exchange sites such as a regular mixture.

From the slopes and intercepts in Figure 11,  $K_{th}$  and  $b$  are calculated and shown in Table 1. Steck and Yeager obtained  $K_H^M (=1/K'$  in eq 20.2) at  $x_{HM} = 0.5$  for Nafion 120 membranes (EW = 1200) with several kinds of mixed cation forms.<sup>9</sup> As seen from eq 28,  $K'(x_{HM}=0.5)$  is identical to  $K_{th}$ , and these values for Nafion 120 are also shown in Table 1. Good conformity is found between  $K_{th}$  in the present work and those values for Nafion 120.  $K_{th}$  is a measure of the interaction between cations and sulfonic acid groups, and  $b$  is a measure of the interaction of  $H^+$  and alkali metal ions  $A^+$  in the mixed state as compared with the state before mixture. Larger  $K_{th}$  means that  $H^+$  has a higher affinity to the sulfonic acid group than  $A^+$  does, which conforms well to the results in Figure 1. Also a more positive value of  $b$  means repulsive (energetically unfavorable) interactions between  $H^+$  and  $A^+$  as compared with the mixture of  $H^+-H^+$  pairs and  $A^+-A^+$  pairs. It is seen in Table 1 that the systems can be classified into two groups, one is with H/Li and H/Na where  $b$  is positive, and the other is with H/K, H/Rb, and H/Cs where  $b$  is negative. Two kinds of classes are observed also in water content  $\lambda$  (Figure 2), membrane density  $d_{wet}$  (Figure 3), water transference coefficient  $t_{H_2O}$  (Figure 7), and water permeability  $L_p$  (Figure 9) expressed as a function of  $x_{HM}$ . How these differences evolve would partly be affected by the presence of water molecules surrounding these cations.

The water molecules surrounding cations may play an important role in several ways, when these cations coexist in

**TABLE 2: Ionic Mobility  $u_i$  and the Parameters Concerning Water in the Ionic Channel<sup>a</sup>**

ion	$\lambda$ in M-form	$t_{\text{H}_2\text{O}}$ in M-form	$K_{\text{th}}$ for $\text{H}^+/\text{M}^+$	$10^8 u_i / \text{m}^2 \text{ V}^{-1} \text{ s}^{-1}$	$10^8 u_i(l) / \text{m}^2 \text{ V}^{-1} \text{ s}^{-1}$
$\text{H}^+$	22.0	2.6	1.00	19.4	36.3
$\text{Li}^+$	24.2	15.8	1.54	3.51	4.01
$\text{Na}^+$	20.0	9.2	0.70	4.50	5.19
$\text{K}^+$	13.1	4.9	0.27	3.45	7.62
$\text{Rb}^+$	10.9	5.5	0.18	2.59	7.92
$\text{Cs}^+$	9.7	5.2	0.15	2.20	7.96

<sup>a</sup> Ionic mobility in the liquid electrolyte at infinite dilution,  $u_i(l)$ , is also cited.<sup>21</sup>

the membrane. Note that the above two classes of systems categorized by  $b$  values are strongly connected with the amount of water in the membrane of relevant cation forms. For the systems H/Li or H/Na, the amount of water is large, and the repulsive force between a pair of alkali metal cations  $\text{A}^+ - \text{A}^+$  would be mitigated by a shielding effect of the water sheath. Here the interaction between cations will become repulsive due to the smaller mutual distance, only if a pair of cations  $\text{H}^+ - \text{A}^+$  are brought into contact. On the other hand, for the systems H/K, H/Rb, and H/Cs, the water content is low and the polymer structure tends to shrink (see Figure 10). In this case the large ions would exert repulsive forces between each other, and the repulsive force between  $\text{H}^+$  and  $\text{A}^+$ , would be smaller than the force between  $\text{H}^+ - \text{H}^+$  or  $\text{A}^+ - \text{A}^+$  averaged for the mixed state.

The way the water content changes by the change in membrane composition, as seen in Figure 2, might also influence the amount of dragged water per charge in mixed cation systems (Figure 7). In the case of H/K, H/Rb, and H/Cs systems, the water content decreases in the mixed state, in contrast to the case of H/Li and H/Na systems. In the former case, some of the water molecules are discarded when the mixture of ions drags water in order to keep high ionic conductivity, as seen in Figure 8. This may also be considered a result of the specific microscopic structure of the membrane, where channels connecting ionic cluster domains are common pathways of both water and cations. In the narrow ionic channels, cations that have a high  $t_{\text{H}_2\text{O}}$  value would suffer a large friction force from the surroundings, and conductivity would become low. In this sense it is interesting to see the order of the largeness of mobility in the membrane, i.e.,  $\text{Li}^+ < \text{Na}^+ > \text{K}^+ > \text{Rb}^+ > \text{Cs}^+$ . The irregularity of the  $\text{Li}^+$  ion can thus be explained, if the large  $t_{\text{H}_2\text{O}}$  value is taken into account.

Table 2 summarizes relevant parameters for ionic mobility and the role of water in ionic channels. Transport characteristics of Nafion membranes are affected differently for different kinds of cation systems. Thereby it is anticipated that three major factors would determine the ion mobility in the membrane:

(1) the larger affinity of cations to the sulfonic acid groups results in smaller cationic mobility,

(2) the smaller water content in the membrane results in smaller cationic mobility, and

(3) the larger  $t_{\text{H}_2\text{O}}$  results in smaller cationic mobility.

(1) is related to the degree of electrostatic interaction, and (2) and (3) are related to the relative size of moving ions and the ionic channel. These factors should be the criteria for designing membranes of higher ionic conductivity, but a more essential factor would be the structural feature of ion channels that are brought about through the hydrophilic–hydrophobic phase separation process of polymer electrolytes.

## 5. Conclusions

The equilibrium and transport characteristics of Nafion membranes were investigated with the binary cation systems

of  $\text{H}^+$  and several kinds of alkali metal cations. The following were found regarding the effects of interactions by such cations and water molecules on the membrane performance.

(1) Except for  $\text{Li}^+$ , alkali metal cations have a higher preference over  $\text{H}^+$  in Nafion membranes.

(2) The polymer electrolyte membrane shrinks and the density increases if the alkali metal cations  $\text{K}^+$ ,  $\text{Rb}^+$ , and  $\text{Cs}^+$  are exchanged for  $\text{H}^+$  in the membrane.

(3) If these cations exist in solutions contacting the membrane, the water content  $\lambda$ , the ionic conductivity  $\kappa$ , ionic transference number of  $\text{H}^+$  in the membrane  $t_{\text{H}^+}$ , and water permeability  $L_p$  decreases steeply as the amount of cations increases.

(4) Two different modes of effects are found for different kinds of cation pairs in  $\lambda$  vs  $x_{\text{HM}}$ ,  $d_{\text{wet}}$  vs  $x_{\text{HM}}$ ,  $L_p$  vs  $x_{\text{HM}}$  and  $t_{\text{H}_2\text{O}}$  vs  $t_{\text{H}^+}$  behaviors. These are ascribed to different interaction modes among ions and water molecules.

(5) Three kinds of factors related to the nature of cations determine their ionic conductivity in the membrane: the affinity to the sulfonic acid groups, the water content in the membrane and water transference coefficients. These factors should be of significant criteria in considering the microstructural designing of high-performance polymer membranes.

## References and Notes

- (1) Srinivasan, S.; Manko, D. J.; Koch, H.; Enayetullah, M. A.; Appleby, J. J. *Power Sources* **1990**, 29, 367.
- (2) Heitner-Wirguin, C. *J. Membr. Sci.* **1996**, 120, 1.
- (3) Verbrugge, M. W.; Hill, R. F. *J. Electrochem. Soc.* **1990**, 137, 886; 893; 1131.
- (4) Cappadonia, M.; Erning, J. W.; Stimming, U. *J. Electroanal. Chem.* **1994**, 376, 189.
- (5) Samec, Z.; Trojánek, A.; Samcová, E. *J. Electroanal. Chem.* **1995**, 389, 1; 25.
- (6) Sone, Y.; Ekdunge, P.; Simonsson, D. *J. Electrochem. Soc.* **1996**, 143, 1254.
- (7) Samec, Z.; Trojánek, A.; Langmaier, J.; Samcová, E. *J. Electrochem. Soc.* **1997**, 144, 4236.
- (8) Lehmani, A.; Turq, P.; Périé, M.; Périé, J.; Simonin, J.-P. *J. Electroanal. Chem.* **1997**, 428, 81.
- (9) Steck, A.; Yeager, H. L. *Anal. Chem.* **1980**, 52, 1215.
- (10) Yeager, H. L. In *Perfluorinated Ionomer Membranes*; Eisenberg, A. E., Yeager, H. L., Eds.; ACS Symposium Series 180; American Chemical Society: Washington, DC, 1982; p 25.
- (11) Bontha, J. R.; Pintauro, P. N. *Chem. Eng. Sci.* **1994**, 49, 3835.
- (12) Samec, Z.; Trojánek, A.; Samcová, E. *J. Phys. Chem.* **1994**, 98, 6352.
- (13) Pourcelly, G.; Sistat, P.; Chapotot, A.; Gavach, C.; Nikonenko, V. *J. Membr. Sci.* **1996**, 110, 69.
- (14) Tandon, R.; Pintauro, P. N. *J. Membr. Sci.* **1997**, 136, 207.
- (15) Yang, Y.; Pintauro, P. N. *AIChE J.* **2000**, 46, 1177.
- (16) Okada, T.; Møller-Holst, S.; Gorseth, O.; Kjelstrup-Ratkje, S. *J. Electroanal. Chem.* **1998**, 442, 137.
- (17) Xie, G.; Okada, T. *Denki Kagaku* **1996**, 64, 718.
- (18) Magnar, O.; Førland, T.; Kjelstrup-Ratkje, S.; Møller-Holst, S. *J. Membr. Sci.* **1992**, 74, 1.
- (19) Kontturi, K.; Ekman, A.; Forssell, P. *Acta Chem. Scand.* **1985**, A39, 273.
- (20) Harned, H. S.; Owen, B. B. *The Physical Chemistry of Electrolytic Solutions*; Reinhold Book Corp.: New York, 1958.
- (21) Conway, B. E. *Electrochemical Data*; Greenwood Press: Westport, CT, 1969.
- (22) Okada, T.; Nakamura, N.; Yuasa, M.; Sekine, I. *J. Electrochem. Soc.* **1997**, 144, 2744.
- (23) Okada, T.; Kjelstrup-Ratkje, S.; Hanché-Olsen, H. *J. Membr. Sci.* **1992**, 66, 179.
- (24) Goswami, A.; Acharya, A.; Pandey, A. K. *J. Phys. Chem. B* **2001**, 105, 9196.
- (25) Fernández-Prini, R.; Philipp, M. *J. Phys. Chem.* **1976**, 80, 2041.
- (26) Okada, T.; Ayato, Y.; Yuasa, M.; Sekine, I. *J. Phys. Chem. B* **1999**, 103, 3315.
- (27) Holt, T.; Førland, T.; Kjelstrup-Ratkje, S. *J. Membr. Sci.* **1985**, 25, 133.
- (28) Førland, K. S.; Okada, T.; Kjelstrup-Ratkje, S. *J. Electrochem. Soc.* **1993**, 140, 634.